Measurements of spatial periodicity and radial structure of NBI-driven Alfvén eigenmodes in the TJ-II stellarator

P. Pons-Villalonga[1], Á. Cappa[1], E. Ascasíbar[1], K. Rahbarnia[2], S. Vaz Mendes[2], C. Bueschel[2], M.B. Dreval[3], O.S. Kozachok[3], O.O. Chmyga[3], J. Varela[4], J. Ortiz[4], and the TJ-II Team[1]

[1]*CIEMAT, Madrid, Spain* [2]*MPI-IPP, Greifswald, Germany*

[3]*IPP NSC KhIPT, Kharkov, Ukraine* [4]*UC3M, Madrid, Spain*

Introduction. Fast particle driven Alfvén eigenmodes (AEs) can be detrimental for plasma heating and plasma facing components, as they can enhance the transport of energetic particles [1]. On the other hand, the artificial excitation of selected eigenmodes has been proposed as a method for ash removal [2]. For these reasons, their study and control in present experimental devices is fundamental for burning plasma operation. To that effect, a new helical array of tri-axial Mirnov coils was recently installed and calibrated in the TJ-II stellarator. This new set of magnetic coils enables the experimental determination of toroidal mode numbers, while enhancing the poloidal mode number determination capabilities of the existing poloidal array.

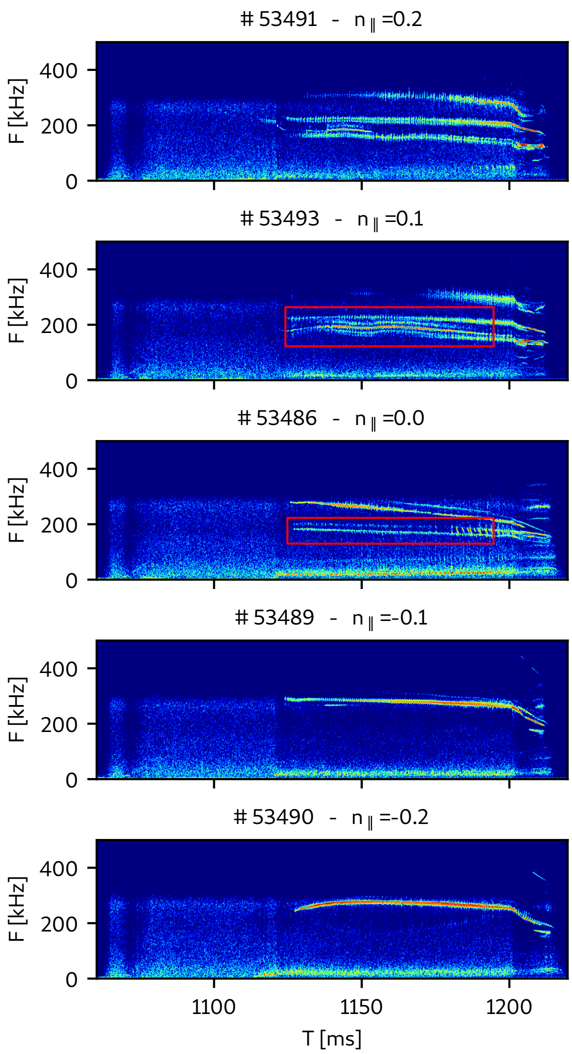

Figure 1: *Mirnov spectrograms of a series of shots with varying ECCD injection angle ($n_\parallel$). In red, the fluctuations analised in this paper.*

During the 2022 campaign the first experiments to test the capabilities of this diagnostic were carried out, using on-axis Electron-Cyclotron Current Drive (ECCD) and Neutral Beam Injection (NBI) to excite an assortment of different eigenmodes. This work describes this experiment and its analysis, focusing on the determination of the spatial periodicity of the observed eigenmodes, and using Heavy Ion Beam Probe (HIBP) data to study the potential profiles of the perturbations. Comparisons with theory have also been carried out.

The experiment. The TJ-II stellarator (heliac, $R_0 = 1.5$ m, $a \leq 0.22$ m, four periods, $B_0 = 0.95$ T, $V \leq 1$ m^3) is an ideal testbed for Alfvén eigenmode characterization. There, the excitation of AEs using NBI has been routinely demonstrated and studied [5]. The new helical array of Mirnov coils, that covers a full period of the device, is comprised of 64 sensors of tri-axial, orthogonal coils, and is described in detail in [3]. It complements the existing 25-coil poloidal array [4] for a total of 217 coils.

The objective of this experiment was to destabilize different AEs to characterize their dependence on plasma current and magnetic configuration, comparing the results with simulations, and to test, verify, and understand the limitations of mode analysis tools (FFT2D, Lomb periodogram [7], SSI-method [8, 9]). To that effect, a scan was made on magnetic configuration, EC beam incidence angle (to modify the current profile and therefore the rotational transform), and NBI injection direction (using co- and counter beams). ECRH is used for plasma startup and then, at lower power, for ECCD and density control; while NBI turns on mid-discharge to provide the fast-particle population that excites the AEs.

The resulting shots present electroO.O.Chmygan temperatures of the order of 1.3 keV, ion temperatures of ~ 120 eV at the plasma core, and low central densities ($\leq 1\times10^{19}$ m^{-3}, typ. $\simeq 0.7\times10^{19}$ m^{-3}), both kept constant during the NBI phase. In figure 1, the Mirnov spectrograms of a series of five shots, with the same configuration and NBI injection direction (counter), but differing in EC injection angle, parametrized by $n_{\parallel}$, the cosine of the angle between the beam and the magnetic axis at their intersection point, are shown. This work will show the analysis of shots #53493 and #53486.

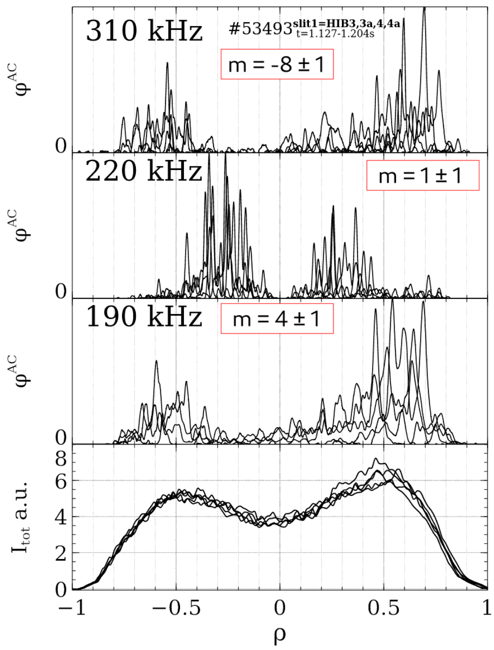

Figure 2: *Radial distribution of the perturbation amplitudes for shot 53493, determined using HIBP*

HIBP. The HIBP data allows us to characterize the radial location of the eigenmodes [6]. This diagnostic performs a radial sweep of the plasma every 15 ms, measuring electric potential, density, and poloidal magnetic field. In figure 2, we can see the potential perturbation amplitude profiles for the three main branches in shot 53493, with 5 overlayed sweeps for the duration of the perturbation ($\sim$80 ms). The perturbations are clearly asymmetric, which may suggest that they are gap modes, produced by the coupling of different mode numbers; and they have maximum amplitudes at different zones in the plasma (HFS for the 220 kHz mode, and LFS for the 190 and 310 kHz ones).

Mode analysis. The mode analysis is done using the Lomb periodogram extension presented in [7], and its results compared with other methods to ensure consistency (see figure 4 for a comparison with the SSI-method). The periodogram fits the data to a sum of sinusoids, with phase given by $m\theta + n\phi - \omega t$, being θ and ϕ the poloidal and toroidal boozer angles on the closest point of the plasma surface to each coil, and returns the normalized difference between the data and the fit. This is shown in figure 3. Although the coils of the poloidal array are arranged in the same vertical plane, their toroidal magnetic angle is not constant, which causes a band structure with nonzero slope to appear on the periodogram (figure 3, top left), generating an uncertainty of ± 1 when determining the poloidal mode number.

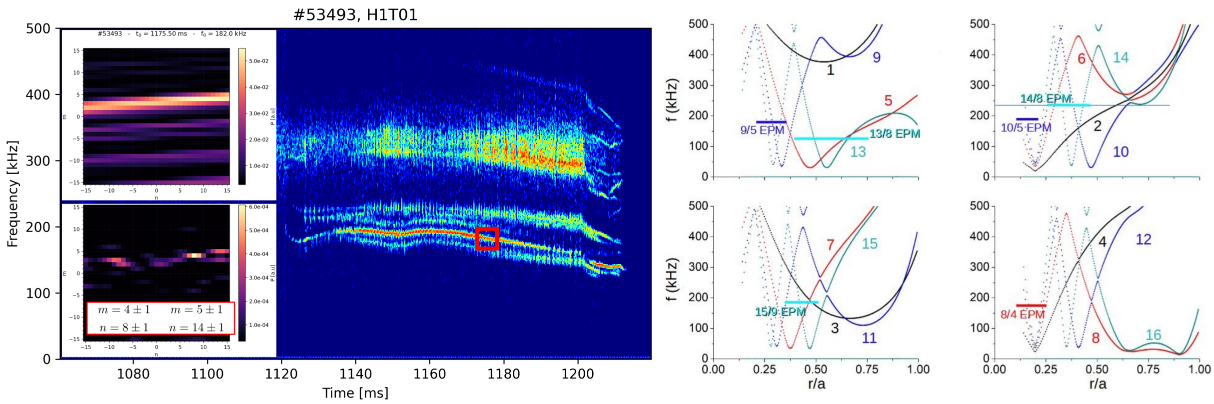

Figure 3: *Mode analysis for the most intense fluctuation branch. Left: Lomb periodograms of the poloidal array (top) and both arrays (bottom) during the time window indicated by the red square on the spectrogram. Right: Alfvén continuum calculated with* `STELLGAP`*, showing the Alfvén continuum gaps with frequencies close to the experimentally observed ones.*

Comparison with theory. The main driver for change in the Alfvén spectrum in this experiment is the plasma current. For this reason, its accurate modeling is needed to obtain meaningful results when carrying out the simulations. There are four components to this current: neutral beam current drive (NBCD), the already mentioned ECCD, bootstrap current, and the induced shielding current. In TJ-II, the NBCD is well understood [12], and its contribution remains constant during the phase of interest. The ECCD current profile is modeled as a narrow gaussian centered on the magnetic axis, and the bootstrap current is neglected, as it is small ($\sim$ 0.1–0.2 kA [12]). The shielding current evolves during the discharge, and is modeled as in [13].

Discussion. This analysis has neglected polarization effects, that may well produce additional phase differences between coils and should be corrected, especially in the helical array. This will be treated in future work. Furthermore, the transfer function between the plasma oscillations and the coil proper is not well understood yet, although some work has recently been done on that topic [14], which could add to the uncertainty in the mode number determination.

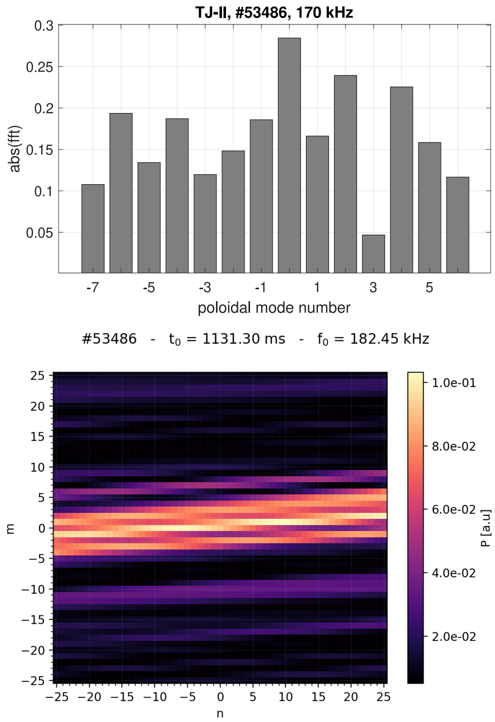

Figure 4: *Poloidal mode number measurement for shot #53486 with SSI (top) and the Lomb periodogram (bottom). Two close-m modes appear, with* $m = 0 \pm 1$ *being the most dominant*

`STELLGAP` and `FAR3D` simulations show that continuum gaps are too narrow and do not get excited, and that the most unstable modes are Energetic Particle Modes (EPMs). However, the radial potential profiles obtained with `FAR3D` are too close to the plasma core to be compatible with the experimental HIBP profiles, which might be caused by a too-steep current profile. A more accurate modeling of the plasma current might improve this agreement.

Acknowledgements. This work has been carried out within the framework of the EUROfusion Consortium, funded by the European Union via the Euratom Research and Training Programme (Grant Agreements No 101052200 and 633053 — EUROfusion). Views and opinions expressed are however those of the author(s) only and do not necessarily reflect those of the European Union or the European Commission. Neither the European Union nor the European Commission can be held responsible for them.

References

[1] L. Chen, F. Zonca, Rev. Mod. Phys. **88**, 015008 (2016)
[2] Ya.I. Kolesnichenko, V.V. Lutsenko *et al.*, Phys. Plasmas **9**, 517 (2002)
[3] E. Ascasíbar *et al.*, Rev. Sci. Instrum. **93**, 093508 (2022)
[4] R. Jiménez-Gómez *et al.*, Fusion Sci. Technol. **51** 20–30 (2007)
[5] Á. Cappa *et al.*, Nucl. Fusion **61** 066019 (2021)
[6] A.V. Melnikov *et al.* Plasma Phys. Control. Fusion **64** 054009 (2022)
[7] S. Zegenhagen *et al.*, Plasma Phys. Control. Fusion **48** 1333 (2006)
[8] R. Kleiber *et al.*, Plasma Phys. Control. Fusion **63** 035017 (2021)
[9] K. Rahbarnia *et al.*, Plasma Phys. Control. Fusion **63** 015005 (2021)
[10] D.A. Spong, R. Sanchez, A. Weller, Phys. Plasmas **10** 3217–3224 (2003)
[11] D.A. Spong *et al.*, Nucl. Fusion **61** 116061 (2021)
[12] S. Mulas *et al.*, Nucl. Fusion **63** 066026 (2023)
[13] M. Zanini *et al.*, Nucl. Fusion **60** 106021 (2020)
[14] C. Bueschel *et al.*, DPG-Frühjahrstagung SMuK, P 11.23 (2023)